PHYSICAL METALLURGY AND HEAT TREATMENT / МЕТАЛЛОВЕДЕНИЕ И ТЕРМИЧЕСКАЯ ОБРАБОТКА

UDC 669.1 : 620.1
https://doi.org/10.17073/0021-3438-2024-1-70-80

Research article
Научная статья

Structure and mechanical properties of PR-03N18K9M5TYu steel grade fabricated by selective laser melting and post-processing

A.O. Kayasova, F.A. Baskov, T.A. Lobova, E.A. Levashov

National University of Science and Technology "MISIS"
4 Bld. 1 Leninskiy Prosp., Moscow 119049, Russia

✉ Anastasiya O. Kayasova (NKayasova@gmail.com)

Abstract: We fabricate samples of PR-03N18K9M5TYu steel (equivalent to ChS4) using selective laser melting (SLM) in a nitrogen atmosphere. Our research focused on the influence of hot isostatic pressing (HIP) combined with heat treatment (HT), specifically hardening and aging, on the steel's structure and its physical and mechanical properties (σ_{ucs}, σ_{ys}, δ, ψ). Through tensile testing, we evaluated the impact of post-processing treatments (HIP followed by HT) on the material's strength. We also assessed how different post-processing protocols affected residual porosity. Our findings indicate that samples exhibiting the highest strength and plastic properties correspond to those with the least structural defects and minimal residual porosity. In-depth microstructural analysis revealed that the optimal structure—a fine-grained, homogeneous configuration—is achieved via the combined application of SLM, HIP, and subsequent HT. The improvement in mechanical properties can be primarily attributed to the dispersed hardening effect, which is a consequence of the precipitation of the superfluous Ni_3Ti phase. Fractographic examination revealed that the post-processing leads to a ductile and dimple fracture, occurring through mechanisms of shearing and detachment, giving rise to mixed-type fractures. The samples that displayed superior mechanical properties were characterized by a homogenous ductile intergranular fracture surface with clear evidence of plastic deformation. We measured the hardness (H), modulus of elasticity (E), and elastic recovery via indentation methods. The post-processing treatments notably enhanced material hardness and elastic modulus, with an increase from $H = 4.6$ GPa and $E = 194$ GPa in the sample post-HIP to $H = 8.5$ GPa and $E = 256$ GPa following HIP coupled with hardening and aging.

Keywords: selective laser melting, maraging steel, hot isostatic pressing, heat treatment, microstructure, mechanical properties.

Acknowledgments: The work was carried out with financial support from the Ministry of Science and Higher Education of the Russian Federation within the framework of a state assignment (project No. 0718-2020-0034).

For citation: Kayasova A.O., Baskov F.A., Lobova T.A., Levashov E.A. Structure and mechanical properties of PR-03N18K9M5TYu steel grade fabricated by selective laser melting and post-processing. *Izvestiya. Non-Ferrous Metallurgy*. 2024;30(1):70–80.
https://doi.org/10.17073/0021-3438-2024-1-70-80

Особенности структуры и механические свойства стали ПР-03Н18К9М5ТЮ, полученной методом селективного лазерного сплавления в сочетании с постобработкой

А.О. Каясова, Ф.А. Басков, Т.А. Лобова, Е.А. Левашов

Национальный исследовательский технологический университет «МИСИС»
Россия, 119049, г. Москва, Ленинский пр-т, 4, стр. 1

✉ Анастасия Олеговна Каясова (NKayasova@gmail.com)

Аннотация: Методом селективного лазерного сплавления (СЛС) в среде азота был получен материал из стали марки ПР-03Н18К9М5ТЮ (аналог ЧС4). Изучено влияние горячего изостатического прессования (ГИП) и термообработки (ТО) – закалки (З) и старения (С) – на структуру и физико-механические свойства ($\sigma_в$, $\sigma_{0,2}$, δ, ψ) СЛС-материала. Для анализа влияния постобработки (ГИП + ТО) на прочностные характеристики проведены испытания на разрыв. Проанализировано изменение остаточной пористости в результате различных режимов постобработки. Установлено повышение прочностных и пластических характеристик материала с наименьшей концентрацией структурных дефектов и минимальной остаточной пористостью. Исследованы микроструктура и изменения, происходящие в материале под влиянием различных технологических режимов термообработки. Мелкозернистая однородная структура, полученная при сочетании СЛС с ГИП и ТО, обеспечивает оптимальные показатели прочностных и пластических свойств материала. Прирост механических свойств обусловлен дисперсным упрочнением в результате выделения избыточной фазы Ni_3Ti. Фрактографический анализ образцов показал, что в результате постобработки разрушение материала происходит по вязко-ямочному механизму путем среза и отрыва с образованием изломов смешанного типа. Изломы образцов, с наилучшими показателями механических свойств, характеризуются однородной поверхностью вязкого внутрезеренного разрушения с выраженными признаками пластической деформации Методом измерительного индентирования определены твердость (H), модуль упругости (E) и степень упругого восстановления. Значения твердости и модуля упругости возрастают от H = 4,6 ГПа и E = 194 ГПа для образца в состоянии ГИП до H = 8,5 ГПа, E = 256 ГПа для образца после ГИП + З + С.

Ключевые слова: селективное лазерное сплавление, мартенситно-стареющая сталь, горячее изостатическое прессование, термическая обработка, микроструктура, механические свойства.

Благодарность: Работа выполнена при финансовой поддержке Министерства науки и высшего образования Российской Федерации в рамках государственного задания (проект № 0718-2020-0034).

Для цитирования: Каясова А.О., Басков Ф.А., Лобова Т.А., Левашов Е.А. Особенности структуры и механические свойства стали ПР-03Н18К9М5ТЮ, полученной методом селективного лазерного сплавления в сочетании с постобработкой. *Известия вузов. Цветная металлургия.* 2024;30(1):70–80. https://doi.org/10.17073/0021-3438-2024-1-70-80

Introduction

Powder maraging steels are distinguished by their high strength and minimal carbon content. The mechanical properties of these steels are enhanced through alloying with elements that substitute for carbon, such as nickel, molybdenum, and cobalt. The notable strength of maraging steels originates from the precipitation of strengthening intermetallic phases. A critical advantage of maraging steels over other steel grades is their resistance to brittle fracture [1—4].

In comparison to other steel grades, maraging steels exhibit superior processability. They demonstrate exceptional hardenability, weldability, ductility, and resistance to cracking upon cooling. The heat treatment (HT) process for maraging steels is straightforward, involving hardening followed by aging, without the occurrence of warping during heat treatment or decarburization after hardening, which could lead to a loss of strength and increased wear. Consequently, maraging steels are highly suitable for machining.

The outstanding performance of maraging steels enables their use in the production of mission-critical components that demand high strength, ductility, and fracture toughness.

Maraging steel powder is characterized by low reflectivity and excellent weldability, making it well-suited for selective laser melting (SLM) [5; 6]. The SLM process enables the creation of products with complex geometries in a single operation, a task that poses challenges for traditional manufacturing techniques.

However, the SLM process may result in incomplete fusion of powder particles, potentially leading to structural defects, residual porosity, and microcracks. These imperfections can diminish the mechanical properties and overall performance of the products. Therefore, the post-processing of SLM products, including hot isostatic pressing followed by heat treatment, is crucial [7—11].

Researchers [12] fabricated SLM samples of $FeCo_{15}Cr_{14}Ni_4Mo_3$ maraging steel and analyzed the material's structure and mechanical properties before and after aging. Under optimized conditions, the SLM steel displayed a tensile strength of 1484 ± 6 MPa and a yield strength of 1376 ± 4 MPa.

Another study [13] focused on maraging steel with a high molybdenum content (15 %), aging the material at 530 °C to initiate dispersion hardening. The steel retained its martensitic structure through the aging process, which also induced a solid solution transformation and the precipitation of nanosized, dispersed Fe_2Mo particles. Consequently, the steel demonstrated exceptional mechanical properties, with a tensile strength of 1978 ± 38 MPa and a relative elongation of 7.36 %.

The strength of this category of steels can be enhanced through heat treatment at temperatures ranging from 480 to 500 °C over several hours. The presence of alloying elements during the aging process facilitates the segregation of hardening phases such as Ni_3Mo, Ni_3Ti,

Ni_3Al, and within the martensite phase. These phases obstruct the Orowan mechanism [14]. In SLM structures, the layer-by-layer fusion of the powder subjects the steel to cyclic reheating, leading to dispersive hardening [15]. Research has demonstrated that HT significantly improves the steel's mechanical properties. By fine-tuning the HT parameters, the desired properties can be achieved. For example, Tan C. et al. [16] explored the impact of aging at t = 490 °C for τ = 6 h and hardening after holding at t = 840 °C (τ = 1 h) on the microstructure and mechanical properties of the 18N300 grade steel. Compared to samples aged post-SLM, those subjected to hardening followed by aging exhibited increased strength and hardness, albeit with a reduction in elongation at break.

This study aims to examine the influence of post-processing treatments, specifically hot isostatic pressing (HIP) and heat treatment, on the structural, physical, and mechanical properties (σ_{ucs}, σ_{ys}, δ, ψ) of the SLM-fabicated materials made from PR-03N18K9M5TYu steel (equivalent to ChS4).

Materials and methods

The samples were fabricated by SLM using PR-03N18K9M5TYu steel powder (Polema, Tula, Russia). The powder's chemical composition is as follows (wt.%):

Fe	base metal	C	0.02
Mo	5.02	Al	0.15
N	18.2	O	0.017
Ti	0.99	N	0.003
Co	8.99		

The powder particle ranged in size from 10 to 63 µm, with size distribution metrics d_{10} = 18.6 µm, d_{50} = 43.2 µm, and d_{90} = 72.9 µm. The bulk density of the powder was 4.378 g/cm^3. he particles were irregularly shaped, some with attached satellites, and up to 65 µm in size. The powder's microstructure featured fine dendrites, notably without any closed gas micropores. (Fig. 1, *c*).

A "Concept Laser M2" (Germany) machine operating in a nitrogen atmosphere, was utilized for the SLM process. Samples were aligned at 0, 45, and 90 degrees relative to the build platform. SLM parameters included a layer thickness of 30 µm, laser power of 180 W, and scanning speed of 600 mm/s. Internal defects and porosity of the samples were examined using computed tomography with an XTH450 LC *X*-ray scanner (Japan).

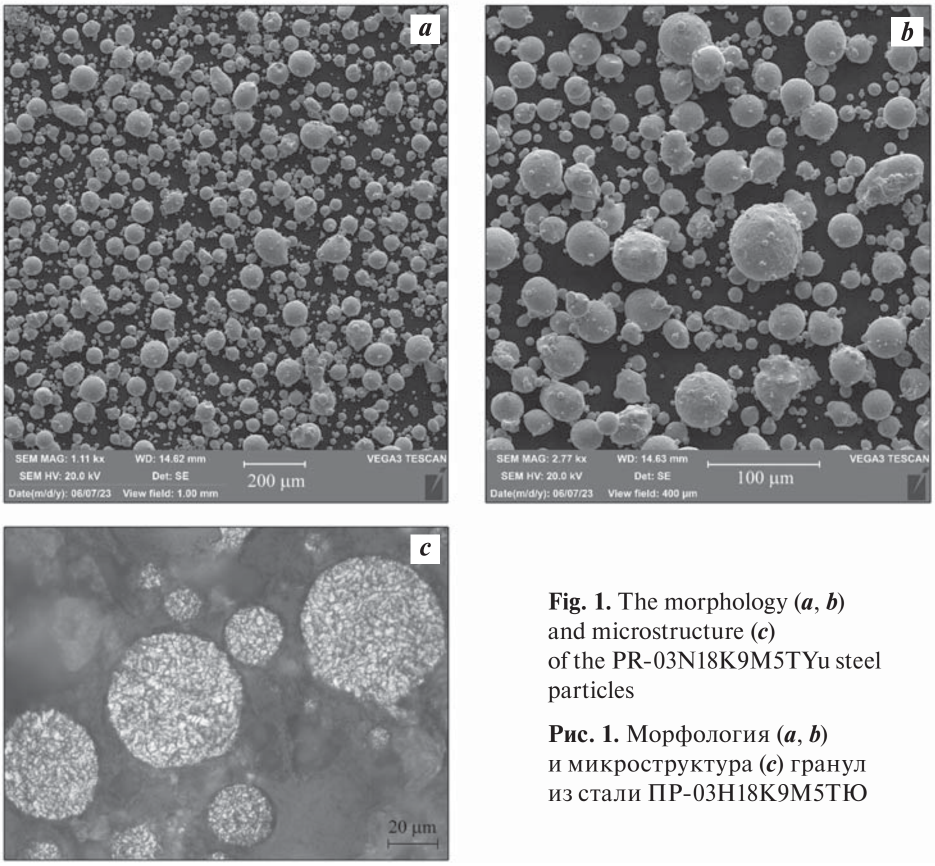

Fig. 1. The morphology (***a***, ***b***) and microstructure (***c***) of the PR-03N18K9M5TYu steel particles

Рис. 1. Морфология (***a***, ***b***) и микроструктура (***c***) гранул из стали ПР-03Н18К9М5ТЮ

The SLM samples underwent HIP using an ABRA HIRP 10/26-200-2000 gasostat (Sweden) in four different modes (HIP1 to HIP4), each with increasing temperature ranges from 920 to 1140 °C, maintained for 2 h at constant pressure. Air quenching followed by aging was performed in an argon-filled electric furnace, with conditions referenced from previous studies [7; 14].

Mechanical properties were assessed by preparing cylindrical tensile test specimens according to GOST 1497-84, type IV, No. 8 standards. A "Shimadzu 100kN" (Japan) tensile test system measured the offset yield strength (σ_{ys}), yield strength (σ_{ucs}), relative elongation (δ), and relative contraction (ψ).

Hardness, elastic modulus, and elastic recovery were determined via indentation using a "Nano-Hardness Tester" (CSM Instruments, Switzerland), applying a 20 mN load to a Berkovich tip, and employing the Oliver—Farr method for plotting loading/unloading curves. Structural investigation employed both scanning electron microscopy (SEM) and transmission electron microscopy (TEM) using an S-3400 (Hitachi, Japan) and a JEM-2100 (JEOL, Japan), respectively, with TEM samples prepared via mechanical thinning and ion beam etching on a PIPS II precision ion polishing system (Gatan, USA). *X*-ray diffraction (XRD) analysis utilized a "Phaser D2" XRD diffractometer (Bruker, USA) with a CuK_α radiation, and energy dispersive spectroscopy was performed with a "NORAN *X*-ray System 7" (Thermo-Fisher Scientific, USA) on the S-3400N electron microscope.

Results and discussion

The SLM process successfully fabricated samples from PR-03N18K9M5TYu steel powder on the build table, as depicted on Fig. 2. *X*-ray tomography analysis revealed no internal defects, such as discontinuities or cracks, within the samples (Fig. 3).

To ascertain the impact of HIP on these samples, tensile tests and porosity analyses were conducted. The initial SLM samples exhibited a porosity level of 0.6 %. Their mechanical properties were measured as follows: an offset yield strength (σ_{ys}) of 1098 MPa, a yield strength (σ_{ucs}) of 1323 MPa, a relative elongation (δ) of 12.6 %, and a relative contraction (ψ) of 42.7 %.

The application of hot isostatic pressing significantly reduced the residual porosity levels to 0.37 % in HIP1 mode, 0.2 % in HIP2, 0.1 % in HIP3, and 0.46 % in HIP4. The combined treatment of HIP with HT (H + A) markedly enhanced the mechanical properties, with increases in σ_{ys} and σ_{ucs}:

— HIP1 + H + A: by 25 % (1335 MPa) and 18 % (1534 MPa), respectively

— HIP2 + H + A: by 26 % (1389 MPa) and 20 % (1590 MPa), respectively

— HIP3 + H + A: by 46 % (1603 MPa) and 35 % (1790 MPa), respectively

— HIP4 + H + A: by 30 % (1430 MPa) and 24 % (1630 MPa), respectively.

These post-processing steps effectively eliminated structural defects and reduced residual porosity, which, in turn, improved the material's strength and plastic

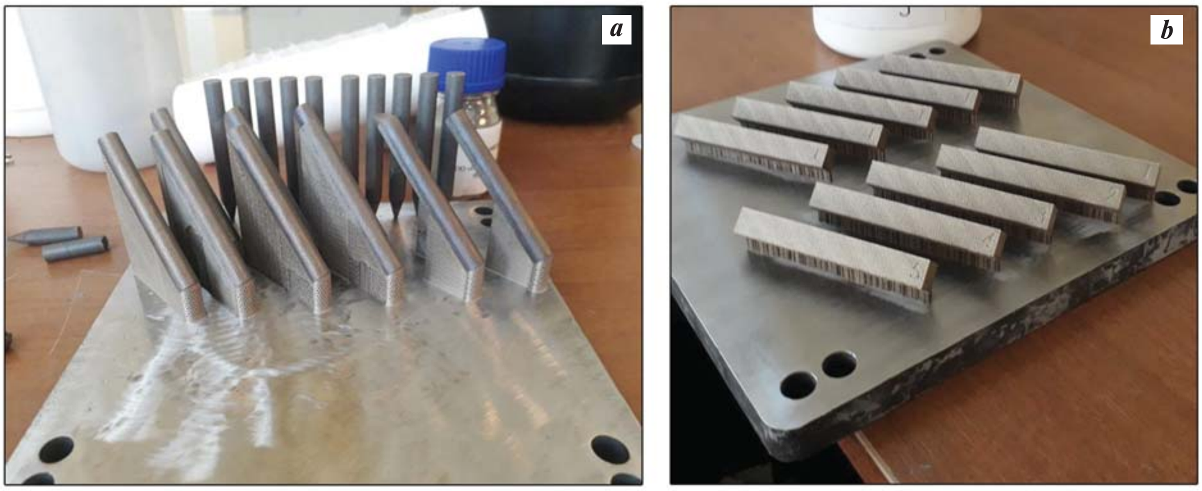

Fig. 2. The SLM samples fabricated from the PR-03N18K9M5TYu steel grade on the build table
a – 45° and 90°; ***b*** – 0°

Рис. 2. Расположение СЛС-образцов из стали ПР-03Н18К9М5ТЮ на платформе построения
a – положение 45° и 90°; ***b*** – положение 0°

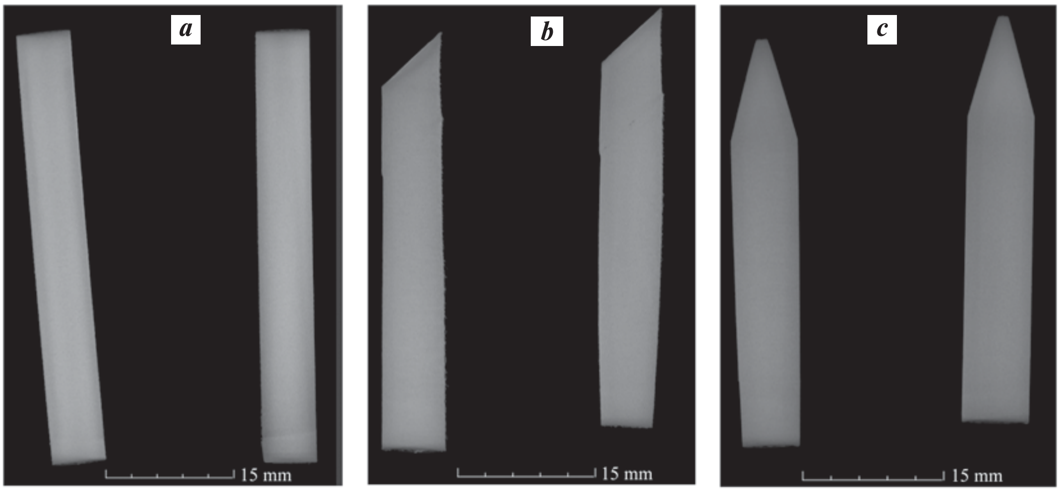

Fig. 3. CT image of the SLM samples
a – 0°; ***b*** – 45°; ***c*** – 90°

Рис. 3. Компьютерная томография СЛС-образцов из стали ПР-03Н18К9М5ТЮ
a – 0°; ***b*** – 45°; ***c*** – 90°

properties. The optimal results in terms of strength and ductility were obtained through the combination of HIP, followed by hardening and aging treatments.

Fig. 4 illustrates the uniaxial strain curves for the samples oriented at 0°, 45°, and 90°, subjected to various post-processing treatments. These curves indicate that the samples possess high strength and plasticity, with a consistent region of plastic deformation. The most favorable outcomes in both plastic and strength properties were achieved with the HIP3 + H + A treatment.

The influence of heat treatment on the material's properties was further confirmed through nanoindentation tests. As shown in Fig. 5 and table, there was a significant increase the hardness (H) and elastic modulus (E) from $H = 4.6$ GPa and $E = 195$ GPa for the sample after HIP, to $H = 8.5$ GPa, $E = 256$ GPa for the sample treated with HIP + H + A.

Fig. 6 depicts the fracture surfaces and the mechanisms of faluer observed in the samples. The prevalent mode of failure is ductile, characterized by dimpling through shearing and detachment, leading to the formation of mixed-type fractures. Some fracture surfaces exhibit pores with diameters up 50 μm.

The fracture morphology of the sample treated with HIP1 + H + A displays heterogeneity, with regions indicative of both brittle and ductile fractures, alongside the presence of micropores. The ductile fracture zones are distinguished by an extensive microrelief, featuring pits and ridges, indicative of significant plastic deformation. Conversely, the sample subjected to HIP3 + H + + A presents a uniformly ductile intergranular fracture surface, with pronounced plastic deformation evidence. The microrelief in this case consists of equiaxed pits, ranging from 5 to 10 μm in size, and notably lacks any signs of brittle fracture.

Microstructure analysis reveals that the samples processed through SLM + HIP + HT exhibit a high degree of structural homogeneity (Fig. 7). The absence of the subgrain structure, typically observed in SLM samples, suggests that grain recrystallization has been completed during post-processing. This structural change enhances mechanical properties through dispersed hardening, resulting from the precipitation of excess Ni_3Ti phase (Fig. 7, *e*), consistent with findings from various studies [7; 17—25].

Conclusions

1. The application of hot isostatic pressing combined with hardening and aging markedly enhances the strength and ductility of SLM-fabricated PR-03N18K9M5TYu steel components. This post-processing approach not only facilitates a sixfold decrease in porosity but also promotes the recrystallization of subgrain structures and induces dispersion hardening.

2. Adjustments in HIP parameters result in a substantial increase in the offset yield strength and tensile strength, specifically between 25 to 46 % and 18 to 35 %, respectively. The combined treatment involving HIP3, followed by hardening and aging, is distinguished by its

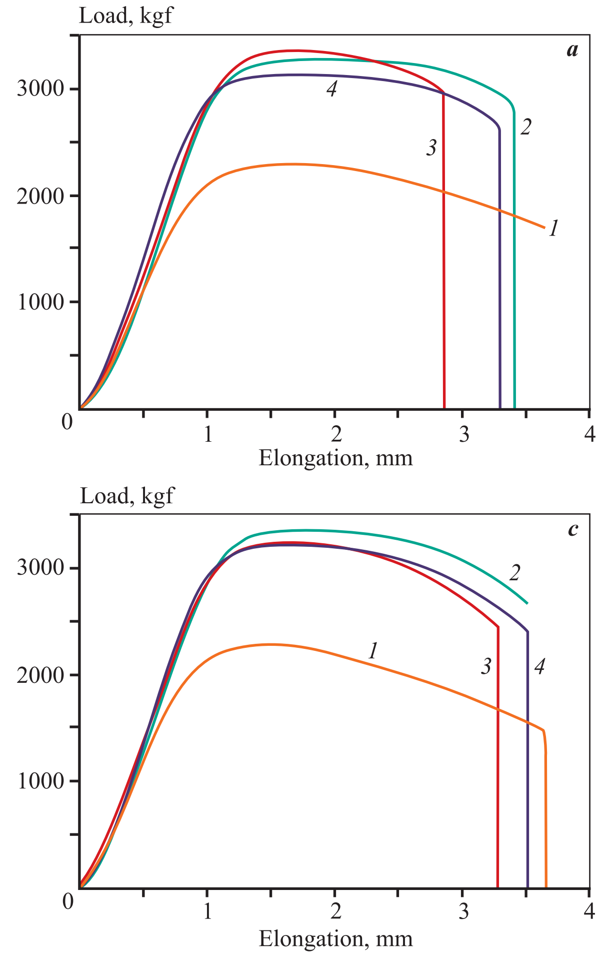

Fig. 4. Uniaxial tensile strain curves

a – 0°, ***b*** – 45°, ***c*** – 90°
1 – HIP1 + H + A; ***2*** – HIP2 + H + A;
3 – HIP3+ H + A; ***4*** – HIP4 + H + A

Рис. 4. Деформационные кривые при одноосном растяжении образцов

a – 0°, ***b*** – 45°, ***c*** – 90°
1 – ГИП1 + З + С; ***2*** – ГИП2 + З + С;
3 – ГИП3+ З + С; ***4*** – ГИП4 + З + С

Hardness (*H*), modulus of elasticity (*E*), and indent depth (h_p)

Значения твердости (H), модуля упругости (E) и глубины отпечатка (h_p)

Sample post-processing	*H*, GPa	*E*, GPa	h_p, nm
HIP1	5.1	209	340
HIP2	4.8	203	342
HIP3	4.6	195	357
HIP4	4.7	196	350
HIP1 + H + A	8.0	240	245
HIP3 + H + A	8.5	256	256

capacity to deliver the highest mechanical performance metric: σ_{ys} = 1603 MPa, σ_{ucs} = 1790 MPa, H = 8 GPa, E = 243 GPa. The fracture mode is primarily ductile with dimple rupture, occurring through mechanisms of shearing and detachment, thus leading to the formation of mixed-type fractures.

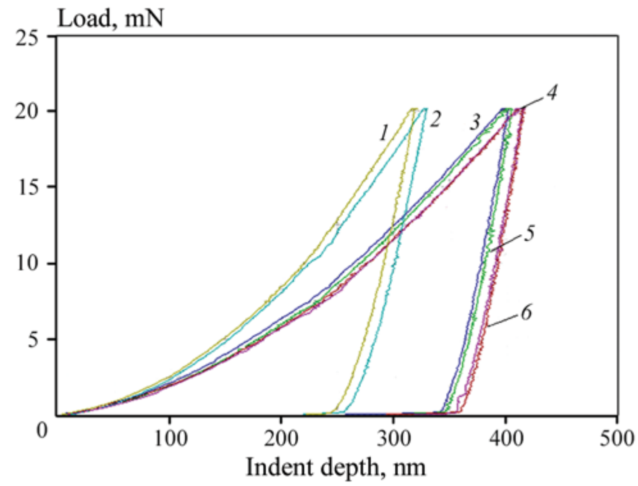

Fig. 5. Loading/unloading curves of samples subjected to various post-processing treatments

1 – HIP1 + H + A; ***2*** – HIP3 + H + A; ***3*** – HIP1; ***4*** – HIP4;
5 – HIP2; ***6*** – HIP3

Рис. 5. Кривые «нагружение – снятие нагрузки» для образцов в различных состояниях

1 – ГИП1 + З + С; ***2*** – ГИП3 + З + С; ***3*** – ГИП1; ***4*** – ГИП4;
5 – ГИП2; ***6*** – ГИП3

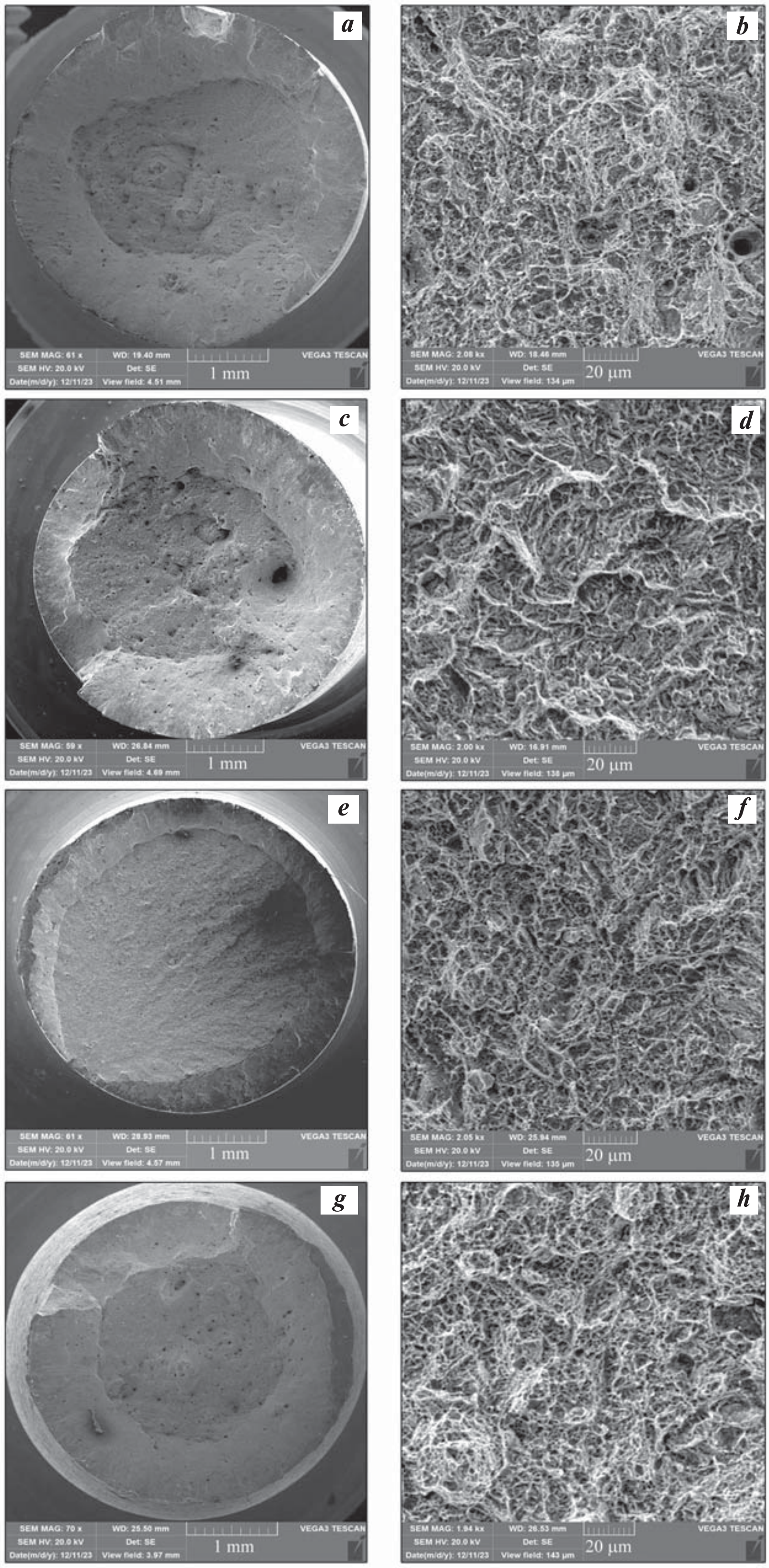

Fig. 6. Samples after HIP1 + H + A (***a***, ***b***), HIP2 + H + A (***c***, ***d***), HIP3 + H + A (***e***, ***f***), HIP4 + H + A (***g***, ***h***)
a, c, e, g – fracture images; ***b, d, f, h*** – fracture surface reliefs

Рис. 6. Образцы в состояниях ГИП1 + З + С (***a***, ***b***), ГИП2 + З + С (***c***, ***d***), ГИП3 + З + С (***e***, ***f***), ГИП4 + З + С (***g***, ***h***)
a, c, e, g – внешний вид излома образца; ***b, d, f, h*** – рельеф поверхности излома

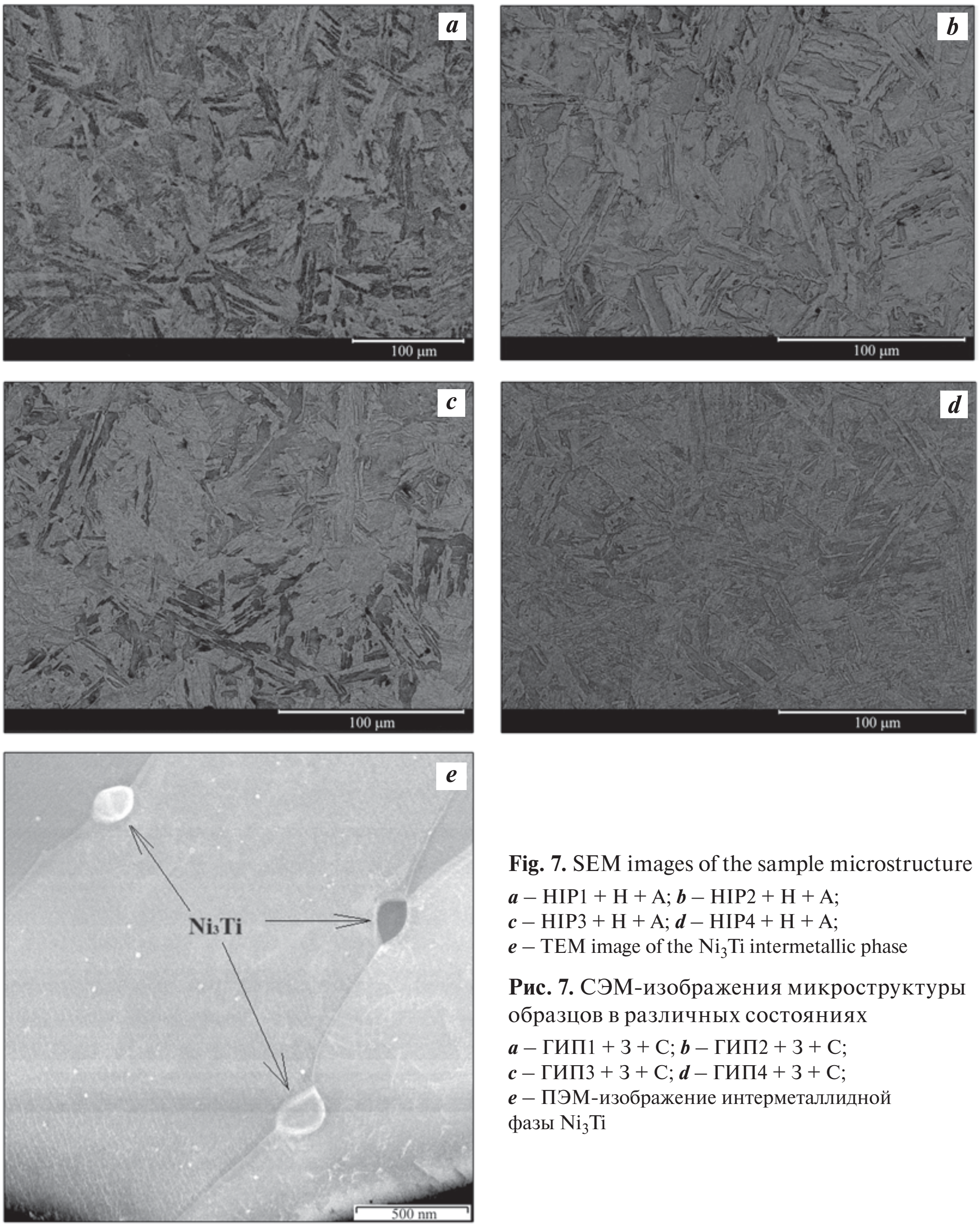

Fig. 7. SEM images of the sample microstructure
a – HIP1 + H + A; ***b*** – HIP2 + H + A;
c – HIP3 + H + A; ***d*** – HIP4 + H + A;
e – TEM image of the Ni_3Ti intermetallic phase

Рис. 7. СЭМ-изображения микроструктуры образцов в различных состояниях
a – ГИП1 + З + С; ***b*** – ГИП2 + З + С;
c – ГИП3 + З + С; ***d*** – ГИП4 + З + С;
e – ПЭМ-изображение интерметаллидной фазы Ni_3Ti

References

1. Ullah R., Akmal J.S. Anisotropy of additively manufactured 18Ni300 maraging steel: threads and surface characteristics. *Procedia CIRP*. 2020;93:68—78. https://doi.org/10.1016/j.procir.2020.04.059
2. Kucerova L., Zetkova I., Jenicek S., Burdova K. Hybrid parts produced by deposition of 18Ni300 maraging steel via selective laser melting on forged and heat treated advanced high strength steel. *Additive Manufacturing*. 2020;32:100—111. https://doi.org/10.1016/j.addma.2020.101108
3. Yuchao Bai, Cuiling Zhao, Jiayi Zhang, Hao Wang. Abnormal thermal expansion behaviour and phase transition of laser powder bed fusion maraging steel with different thermal histories during continuous heating. *Additive Manufacturing*. 2022;53:102712. https://doi.org/10.1016/j.jsis.2019.01.003
4. Dinghui Liu, Jie Su, Ao Wang, Zhuoyue Yang, Jiaoxi Yang, Zhen Wang, Yali Ding, Geng Liu. Tailoring the microstructure and mechanical properties of FeCrNiCoMo maraging stainless steel after laser melting deposition. *Materials Science and Engineering: A*. 2022;840:142931. https://doi.org/10.1016/j.jsis.2019.01.003

5. Vishwakarma J., Chattopadhyay K., Santhi Srinivas N.C. Effect of build orientation on microstructure and tensile behaviour of selectively laser melted M300 maraging steel. *Materials Science and Engineering: A*. 2020; 798:140130.
https://doi.org/10.1016/j.msea.2020.140130
6. Souza A.F., Al-Rubaie K.S., Marques S., Zluhan B., Santos E.C. Effect of laser speed, layer thickness, and part position on the mechanical properties of maraging 300 parts manufactured by selective laser melting. *Materials Science and Engineering: A*. 2019;767:138425.
https://doi.org/10.1016/j.msea.2019.138425
7. Kayasova A.O., Levashov E.A. Features of the impact of hot isostatic pressing and heat treatment on the structure and properties of maraging steel obtained by selective laser melting method. *Powder Metallurgy and Functional Coatings*. 2022;16(4):84—92. (In Russ.).
http://doi.org/10.17073/1997-308X-2022-4-84-92
Каясова А.О., Левашов Е.А. Особенности влияния горячего изостатического прессования и термообработки на структуру и свойства мартенситно-стареющей стали, полученной методом селективного лазерного сплавления. *Известия вузов. Порошковая металлургия и функциональные покрытия*. 2022;16(4):84—92.
http://doi.org/10.17073/1997-308X-2022-4-84-92
8. Kaplanscky Yu.Yu., Levashov E.A., Korotitskiy A.V., Loginov P.A., Sentyurina Zh.A., Mazalov A.B. Influence of aging and HIP treatment on the structure and properties of NiAl-based turbine blades manufactured by laser powder bed fusion. *Additive Manufacturing*. 2020;31:100999.
https://doi.org/10.1016/j.addma.2019.100999
9. Sentyurina Zh.A., Baskov F.A., Loginov P.A., Kaplanskii Yu.Yu. Mishukov A.V. Logachev I.A., Bychkova M.Ya., Levashov E.A. Logacheva A.I. The effect of hot isostatic pressing and heat treatment on the microstructure and properties of EP741NP nickel alloy manufactured by laser powder bed fusion. *Additive Manufacturing*. 2021.37:101629.
https://doi.org/10.1016/j.addma.2020.101629
10. Kaplanskii Yu.Yu., Sentyurina Zh.A., Loginov P.A., Levashov E.A., Korotitskiy A.V., Travyanov A.Ya., Petrovskii P.V. Microstructure and mechanical properties of the (Fe, Ni)Al-based alloy produced by SLM and HIP of spherical composite powder. *Materials Science and Engineering: A*. 2019;743:567—580.
https://doi.org/10.1016/j.msea.2018.11.104
11. Baskov F.A., Sentyurina Zh.A., Kaplanskii Yu.Yu., Logachev I.A., Semerich A.S., Levashov E.A. The influence of post heat treatments on the evolution of microstructure and mechanical properties of EP741NP nickel alloy produced by laser powder bed fusion. *Materials Science and Engineering: A*. 2021;817:141340.
https://doi.org/10.1016/j.msea.2021.141340
12. Conde F.F., Escobar J.D., Oliveira J.P., Jardini A.L., Bose Filho W.W., Avila J.A. Austenite reversion kinetics and stability during tempering of an additively manufactured maraging 300 steel. *Additive Manufacturing*. 2019;29:100804.
https://doi.org/10.1016/j.addma.2019.100804
13. Xu T.Z., Zhang S., Du Y., Wu C.L., Zhang C.H., Sun X.Y., Chen H.T., Chen J. Development and characterization of a novel maraging steel fabricated by laser additive manufacturing. *Materials Science and Engineering: A*. 2024;891:145975.
https://doi.org/10.1016/j.msea.2023.145975
14. Mouritz A.P. 11 — Steels for aircraft structures. In: *Introduction to aerospace material*. Woodhead Publishing, 2012. P. 232—250.
https://doi.org/https://doi.org/10.1533/9780857095152.232
15. Kürnsteiner P., Wilms M.B., Weisheit A., Barriobero-Vila P., Jägle E.A., Raabe D. Massive nanoprecipitation in an Fe—19Ni—*x*Al maraging steel triggered by the intrinsic heat treatment during laser metal deposition. *Acta Materialia*. 2017;129:52—60.
https://doi.org/10.1016/j.actamat.2017.02.069
16. Tan C., Zhou K., Ma W., Zhang P., Liu M., Kuang T. Microstructural evolution, nanoprecipitation behavior and mechanical properties of selective laser melted high-performance grade 300 maraging steel. *Materials & Design*. 2017;134:23—34.
https://doi.org/10.1016/j.matdes.2017.08.026
17. Karolczuk Aleksander, Kurek Andrzej, Böhm Michał, Derda Szymon, Prażmowski Mariusz, Kluger Krzysztof, Żak Krzysztof, Pejkowski Łukasz, Seyda Jan. Heterogeneous effect of aging temperature on the fatigue life of additively manufactured thin-walled 18Ni300 maraging steel tubular specimen. *Materials & Design*. 2024;237:112561.
https://doi.org/10.1016/j.matdes.2023.112561
18. Jonghyun Jeong, Gun Woo No, Hyo Ju Bae, Sang Kyu Yoo, In-Chul Choi, Hyoung Seop Kim, Jae Bok Seol, Jung Gi Kim. Mechanical properties of lamellar-structured 18Ni300 maraging steel manufactured via directed energy deposition. *Materials Science and Engineering: A*. 2024;892:146031.
https://doi.org/10.1016/j.msea.2023.146031
19. Sha W., Guo Z., Wilson E.A. Modeling the evolution of microstructure during the processing of maraging steels, *JOM*. 2004; 56:62—66.
https://doi.org/10.1007/s11837-004-0037-2
20. Moshka O., Pinkas M., Brosh E., Ezersky V., Meshi L. Addressing the issue of precipitates in maraging steels —

unambiguous answer. *Materials Science and Engineering: A*. 2015;638:232—239
https://doi.org/10.1016/j.msea.2015.04.067

21. Zhonghui Cheng, Shengzhi Sun, Xi Du, Qing Tang, Jinguang Shi, Xiaofeng Liu, Qiu Jianrong. Microstructural evolution of a FeCo15Cr14Ni4Mo3 maraging steel with high ductility prepared by selective laser melting. *Materials Today Communications*. 2022;31:103243.
https://doi.org/10.1016/j.mtcomm.2022.103243
22. Lulu Guo, Lina Zhang, Joel Andersson, Olanrewaju Ojo. Additive manufacturing of 18 % nickel maraging steels: Defect, structure and mechanical properties: A review. *Journal of Materials Science & Technology*. 2022;120:227—252.
https://doi.org/10.1016/j.jmst.2021.10.056
23. Yuchao Bai, Di Wang, Yongqiang Yang, Hao Wang. Effect of heat treatment on the microstructure and mechanical properties of maraging steel by selective laser melting. *Materials Science and Engineering: A*. 2019;760: 105—117.
https://doi.org/10.1016/j.msea.2019.05.115
24. Vishwakarma Jaydeep, Chattopadhyay K., Santhi Srinivas N.C. Effect of build orientation on microstructure and tensile behaviour of selectively laser melted M300 maraging steel. *Materials Science and Engineering: A*. 2020;798:140130.
https://doi.org/10.1016/j.msea.2020.140130
25. Habassi Faiçal, Houria Manel, Barka Noureddine, Jahazi Mohammad. Influence of post-treatment on microstructure and mechanical properties of additively manufactured C300 maraging steel. *Materials Characterization*. 2023;202:112980.
https://doi.org/10.1016/j.matchar.2023.112980

Information about the authors

Anastasiya O. Kayasova – Postgraduate Student, Department of Powder Metallurgy and Functional Coating (PM&FC), National University of Science and Technology "MISIS" (NUST MISIS).
https://orcid.org/0009-0009-2144-0332
E-mail: NKayasova@gmail.com

Fedor A. Baskov – Cand. Sci. (Eng.), Researcher, Laboratory "In situ diagnostics of structural transformations", Scientific-Educational Center of SHS of MISIS–ISMAN, NUST MISIS.
https://orcid.org/0000-0001-6238-4378
E-mail: baskov_fa@mail.ru

Tamara A. Lobova – Dr. Sci. (Eng.), Prof. of the Department of PM&FC, NUST MISIS.
https://orcid.org/0009-0002-1749-0782
E-mail: smazka39@mail.ru

Evgeny A. Levashov – Dr. Sci. (Eng.), Prof., Acad. of the Russian Academy of Natural Science, Head of the Department of PM&FC of NUST MISIS, Head of the Scientific-Educational Center of SHS of MISIS–ISMAN.
https://orcid.org/0000-0002-0623-0013
E-mail: levashov@shs.misis.ru

Информация об авторах

Анастасия Олеговна Каясова – аспирант кафедры «Порошковая металлургия и функциональные покрытия» (ПМиФП) Национального исследовательского технологического университета «МИСИС» (НИТУ МИСИС).
https://orcid.org/0009-0009-2144-0332
E-mail: NKayasova@gmail.com

Федор Алексеевич Басков – к.т.н., науч. сотрудник лаборатории «In situ диагностика структурных превращений» Научно-учебного центра (НУЦ) СВС МИСиС–ИСМАН, НИТУ МИСИС.
https://orcid.org/0000-0001-6238-4378
E-mail: baskov_fa@mail.ru

Тамара Александровна Лобова – д.т.н., профессор кафедры ПМиФП, НИТУ МИСИС.
https://orcid.org/0009-0002-1749-0782
E-mail: smazka39@mail.ru

Евгений Александрович Левашов – д.т.н., проф., акад. РАЕН, заведующий кафедрой ПМиФП НИТУ МИСИС, директор НУЦ СВС МИСИС–ИСМАН.
https://orcid.org/0000-0002-0623-0013
E-mail: levashov@shs.misis.ru

Contribution of the authors

A.O. Kayasova – formulated the problem statement, created SLM samples and prepared the samples for additional analysis, performed heat treatment, and authored the manuscripte.

F.A. Baskov – provided guidance on the optimal conditions for HIP, performed the HIP process, and contributed to discussions.

T.A. Lobova – assisted with the SEM studies, analysis of the results, and participated in discussions.

E.A. Levashov – provided general supervision of the study and writing the paper, engaged in discussions.

Вклад авторов

А.О. Каясова – определение цели работы, изготовление СЛС-образцов, подготовка образцов для дальнейших исследований, проведение термической обработки, написание статьи.

Ф.А. Басков – консультирование при выборе параметров ГИП, проведение ГИП, участие в обсуждении результатов.

Т.А. Лобова – помощь при СЭМ-исследованиях, помощь с анализом полученных результатов, участие в обсуждении результатов.

Е.А. Левашов – общее руководство работой, помощь в написании статьи, участие в обсуждении результатов.

The article was submitted 1.01.2024, revised 13.02.2024, accepted for publication 19.02.2024

Статья поступила в редакцию 31.01.2024, доработана 13.02.2024, подписана в печать 19.02.2024